Conceptual Themes for the 2017 Sagan Summer Workshop

Authors: Jennifer C. Yee (SAO) & Calen B. Henderson (JPL)

Theme 1: The Scale of the Einstein Ring

Microlensing is most sensitive to planets near the Einstein ring. Thus, the size of the Einstein ring is fundamental to understanding the type of planets microlensing can find. The key concept is that the size of the Einstein ring scales as the square root of the mass of the host star. The most relevant formulation of the Einstein ring is its size in the lens plane because this corresponds to the typical projected separation of a planet detected by microlensing:

$$r_{\rm E} = \sqrt{\kappa M_\ell \frac{D_\ell (D_\ell - D_s)}{D_s}}, \text{where } \kappa = 8.14 \text{ mas}/M_\odot, \tag{1}$$

for a host star mass M_ℓ in solar masses and distance D_ℓ in kpc and a source at $D_s = 8$ kpc. For most practical purposes, the source can always be assumed to be at approximately 8 kpc. Below is a table showing how the size of the Einstein ring (in AU) scales with the mass and distance of the lens.

Other ways to think about the Einstein ring are in terms of its angular size, $\theta_{\rm E}$, or its physical projection onto the observer plane, $\tilde{r}_{\rm E}$. Typical order-of-magnitude values are 1 mas and 10 AU, respectively. Tables for varying lens (host) masses and distances are given below. The angular size of the Einstein ring is relevant for estimating the separations between the two images and other angular scales on the sky. The projection of the Einstein ring on the observer plane is used for understanding the relative scale of parallax signals, which are induced by the observer.

Useful References on the Scale of Astrometric Microlensing:

- Dominik & Sahu (1998) — Outlines the theory of astrometric microlensing. Figures 1 and 2 Show the scale of the signal relative to the size of the Einstein ring. [`http://adsabs.harvard.edu/abs/1998astro.ph..5360D`]
- Han & Jeong (1999) — The effect of a luminous lens on the astrometric microlensing signal. Figure 1 shows that the astrometric signal decreases as light from non-source stars increases. [`http://adsabs.harvard.edu/abs/1999MNRAS.309..404H`]
- Lu et al. (2016) — Results from a multi-year program using NIRC2 on Keck to measure the centroid shifts of long-timescale microlensing events potentially arising from stellar remnant lenses. [`http://adsabs.harvard.edu/abs/2016ApJ...830...41L`]
  - Fig. 1 [L]: Magnification and centroid shift as a function of tau
  - Fig. 1 [R]: Centroid shift as a function of u (for various M_ℓ); but no (x,y) component analysis
  - S. 2: Overview of the derivation (with refs!) of the centroid shift as f(t_0, $t_{\rm E}$, u_0)

Table 1. Physical Einstein radius $r_{\rm E}$ [AU] for a grid of $(D_\ell,\, M_\ell)^a$

Lens Type	$\boldsymbol{M_\ell}$ $[\boldsymbol{M_\odot}]$	$\boldsymbol{D_\ell}$ **[kpc]**						
		1.0	2.0	3.0	4.0	5.0	6.0	7.0
Black hole	10	8.44	11.05	12.35	12.76	12.35	11.05	8.44
G Dwarf	1	2.67	3.49	3.91	**4.03**	3.91	3.49	2.67
M Dwarf	0.3	1.46	1.91	2.14	**2.21**	2.14	1.91	1.46
M Dwarf	0.1	0.84	1.10	1.23	1.28	1.23	1.10	0.84
Brown Dwarf	0.01	0.27	0.35	0.39	0.40	0.39	0.35	0.27
Jupiter	0.001	0.08	0.11	0.12	0.13	0.12	0.11	0.08

[a]Assuming a source star distance of $D_s = 8$ kpc.

Table 2. Angular Einstein radius $\theta_{\rm E}$ [mas] for a grid of $(D_\ell,\, M_\ell)^a$

Lens Type	$\boldsymbol{M_\ell}$ $[\boldsymbol{M_\odot}]$	$\boldsymbol{D_\ell}$ **[kpc]**						
		1.0	2.0	3.0	4.0	5.0	6.0	7.0
Black hole	10	8.44	5.52	4.12	3.19	2.47	1.84	1.21
G Dwarf	1	2.67	1.75	1.30	**1.01**	0.78	0.58	0.38
M Dwarf	0.3	1.46	0.96	0.71	**0.55**	0.43	0.32	0.21
M Dwarf	0.1	0.84	0.55	0.41	0.32	0.25	0.18	0.12
Brown Dwarf	0.01	0.27	0.17	0.13	0.10	0.08	0.06	0.04
Jupiter	0.001	0.08	0.06	0.04	0.03	0.02	0.02	0.01

[a]Assuming a source star distance of $D_s = 8$ kpc.

Table 3. Projected physical Einstein radius $\tilde{r}_{\rm E}$ [AU] for a grid of (D_ℓ, M_ℓ)[a]

Lens Type	$\boldsymbol{M_\ell}$ [$\boldsymbol{M_\odot}$]	$\boldsymbol{D_\ell}$ **[kpc]**						
		1.0	2.0	3.0	4.0	5.0	6.0	7.0
Black hole	10	9.64	14.73	19.76	25.51	32.93	44.18	67.49
G Dwarf	1	3.05	4.66	6.25	**8.07**	10.41	13.97	21.34
M Dwarf	0.3	1.67	2.55	3.42	**4.42**	5.70	7.65	11.69
M Dwarf	0.1	0.96	1.47	1.98	2.55	3.29	4.42	6.75
Brown Dwarf	0.01	0.30	0.47	0.62	0.81	1.04	1.40	2.13
Jupiter	0.001	0.10	0.15	0.20	0.26	0.33	0.44	0.67

[a]Assuming a source star distance of $D_s = 8$ kpc.

Theme 2: Timescales in Microlensing

The Einstein timescale, $t_{\rm E}$, is the time it takes for the angular separation between the lens and source in the plane of the sky to change by one Einstein radius. In exoplanetary microlensing the standard convention is to keep the lens system fixed (except in the cases wherein there is detectable lens orbital motion) and subsume all of the lens-source relative motion into the trajectory of the source. Therefore, $t_{\rm E}$ can be calculated from the angular size of the Einstein ring and the relative proper motion between the source and the lens stars, $\mu_{\rm rel}$:

$$t_{\rm E} = \theta_{\rm E}/\mu_{\rm rel}. \tag{2}$$

For a bulge lens, $\mu_{\rm rel}$ is typically 4 mas/yr, so a typical value for $t_{\rm E}$ is 30 days. However, it is evident from the above equation that since the Einstein ring scales as the square root of the lens mass, the Einstein timescale also scales as the square root of the lens mass. A table of Einstein timescales for different host masses is given below assuming a source-lens relative proper motion of 4 mas/yr.

In addition to the Einstein timescale, which reflects a single lens (stellar) microlensing event, one might also consider the timescale of planetary perturbations and also the source self-crossing time, t_*. The duration of planetary perturbations varies widely depending on the caustics, but typical timescales are:

The source self-crossing time is the amount of time it takes the source star to travel one source radius:

$$t_* = \theta_*/\mu_{\rm rel}. \tag{3}$$

This sets the timescale of finite source effects in microlensing. Typical values are 1 hour. **These timescales matter because they set the cadence of observations required to characterize the microlensing light curve.**

Table 4. Timescale $t_{\rm E}$ [d] for a grid of (D_ℓ, M_ℓ), assuming $\mu_{\rm rel} = 4$ mas/yr (bulge lens)[a]

Lens Type	$\boldsymbol{M_\ell}$ [$\boldsymbol{M_\odot}$]	$\boldsymbol{D_\ell}$ [**kpc**]						
		1.0	2.0	3.0	4.0	5.0	6.0	7.0
Black hole	10					225.5	168.1	110.1
G Dwarf	1					71.3	**53.2**	34.8
M Dwarf	0.3					39.1	**29.1**	19.1
M Dwarf	0.1					22.6	16.8	11.0
Brown Dwarf	0.01					7.1	5.3	3.5
Jupiter	0.001					2.3	1.7	1.1

[a]Assuming a source star distance of $D_s = 8$ kpc.

Table 5. Timescale $t_{\rm E}$ [d] for a grid of (D_ℓ, M_ℓ), assuming $\mu_{\rm rel} = 10$ mas/yr (disk lens)[a]

Lens Type	$\boldsymbol{M_\ell}$ [$\boldsymbol{M_\odot}$]	$\boldsymbol{D_\ell}$ [**kpc**]						
		1.0	2.0	3.0	4.0	5.0	6.0	7.0
Black hole	10	308.1	201.7	150.4	116.5	90.2		
G Dwarf	1	97.4	63.8	47.5	**36.8**	28.5		
M Dwarf	0.3	53.4	34.9	26.0	**20.2**	15.6		
M Dwarf	0.1	30.8	20.2	15.0	11.6	9.0		
Brown Dwarf	0.01	9.7	6.4	4.8	3.7	2.9		
Jupiter	0.001	3.1	2.0	1.5	1.2	0.9		

[a]Assuming a source star distance of $D_s = 8$ kpc.

Table 6. Timescale of planetary perturbation

Planet	Mass ratio q^a	Timescale
Jupiter	$1 \cdot 10^{-3}$	$\sim$1 d
Neptune	$5 \cdot 10^{-5}$	hours
Earth	$3 \cdot 10^{-6}$	$\sim$1 hr

[a]Assuming a host star with $M_* \sim 1.0 M_\odot$.

Theme 3: Microlensing Planet Observables

As with all planet-finding techniques, the planetary parameters that are measured in microlensing are measured as relative quantities. The two main parameters that characterize a planet are the mass ratio, q:

$$q = M_p/M_*, \tag{4}$$

and the separation, s:

$$s = a_\perp/r_{\rm E}, \tag{5}$$

where $a_\perp$ is the projection of the planet's position onto the lens plane (i.e., we cannot measure the distance in or out of the plane of the star) and $r_{\rm E}$ is the size of the Einstein ring. Hence, to gain intuition for planets in the context of microlensing, q, s, and the size of the Einstein ring are the most critical parameters.

Table 7. Mass ratio q for Solar System bodies

Object	$\boldsymbol{M_*}$ $[\boldsymbol{M_\odot}]$	
	0.3	1.0
Jupiter	3.2e-03	9.5e-04
Saturn	9.5e-04	2.9e-04
Neptune	1.7e-04	5.1e-05
Earth	1.0e-05	3.0e-06
Mars	1.1e-06	3.2e-07
Ganymede	2.5e-07	7.5e-08
The Moon	1.2e-07	3.7e-08

Table 8. Separation s for Solar System planets[a]

Planet	$\boldsymbol{a}$ **[AU]**	$\boldsymbol{D_\ell}$ **[kpc]**	
		4.0	6.0
Neptune	30.07	7.45	8.61
Uranus	19.19	4.76	5.49
Jupiter	9.54	**2.36**	**2.73**
Saturn	5.20	1.29	1.49
Mars	1.52	0.38	0.44
Earth	1.00	0.25	0.29
Venus	0.72	0.18	0.21
Mercury	0.39	0.10	0.11

[a]Assuming a host star with $M_* \sim 1.0 M_\odot$.

Theme 4: The Observer, Lens, and Source Planes

In microlensing, we have three key planes: the observer plane, the lens plane, and the source plane. All of these are parallel to the plane of the sky. Different microlensing effects act in different planes, and therefore, the relevant version of the Einstein ring is different for the different effects.

Topics for which the planes are relevant:

- Planets should be in the lens plane to be detectable; $r_{\rm E}$ as compared to $a_\perp$ is the relevant scale.
- Parallax is an effect measured in the observer plane; $\tilde{r}_{\rm E}$ as compared to $D_\perp$ is the relevant scale.
- Lens orbital motion is measured in the lens plane; $r_{\rm E}$ is the relevant scale.
- Binary sources/xallarap/source orbital motion all relate to the source plane.

In addition, keep in mind that everything we measure is projected onto the plane in question. We don't know the inclination of a lens system; we only know the projected separation between the bodies. We only care about the projection of the Earth and satellite positions onto the plane of the sky when considering parallax.

Theme 5: Caustics and Light Curves

Caustics (and the underlying magnification map) are critical to interpreting microlensing light curves. Some key terms we use for caustics are:

- Types of caustics: planetary, central, resonant
- Caustic features: cusps, folds (non-intersecting and closed morphology for two-body lens systems)
- Light curve features from caustics:
  - caustic crossing, caustic entrance, caustic exit
  - cusp crossing, cusp approach
- Finite-source effects (i.e., relation between finite angular size of source and light curve features)

Throughout the workshop we should be sure to point these features out explicitly in light curves and show the correspondence between the light curve features and the caustic structures.

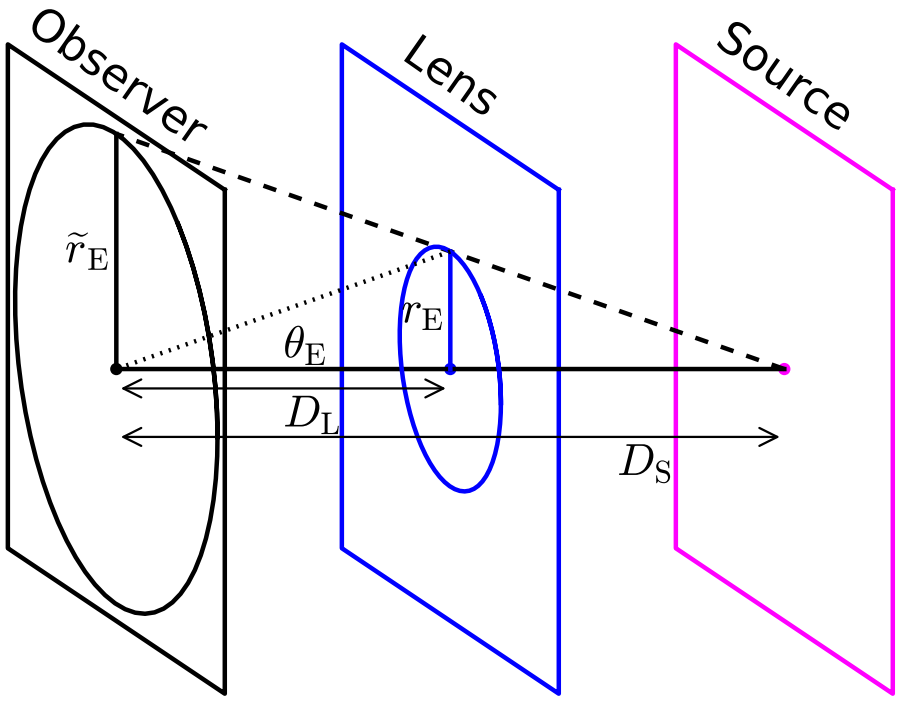

Figure 1 The three relevant planes for gravitational microlensing searches for exoplanets (and lensing phenomena generally). The source star, residing in its eponymous plane, is located at a distance D_s from the observer. In the plane of the lens, $r_{\rm E}$ defines the physical size of the Einstein radius while $\theta_{\rm E}$ defines its angular scale as measured from the observer. Finally, $\tilde{r}_{\rm E}$ identifies the physical size of the Einstein radius projected onto the plane of the observer. Understanding the geometric relations between these three planes is fundamental to developing intuition regarding the inherent sensitivity and limitations of microlensing to exoplanetary systems with different physical parameters.

Theme 6: Physical Properties from Mass-Distance Relations

Because the microlensing relations all involve combinations of M_ℓ and D_ℓ, measuring either one of them necessarily requires measuring two parameters and it also necessarily means measuring both of them. There are three different observables that give mass-distance relations:

- angular Einstein radius $\theta_{\rm E}$
- microlens parallax $\pi_{\rm E}$
- lens flux F_ℓ

Throughout the workshop, we want to emphasize the mass-distance relations that arise from each of these measurements and that the measurement of the lens mass and distance comes from the intersection of two different relations. A good way to show this is to use a Mass-Distance plot similar to the figures in Yee+2015 or Batista+2014 (see below) that show these relations and their intersections. Including uncertainties in these relations would help show how uncertainties in the observables propagate through to uncertainties in the derived mass and distance.

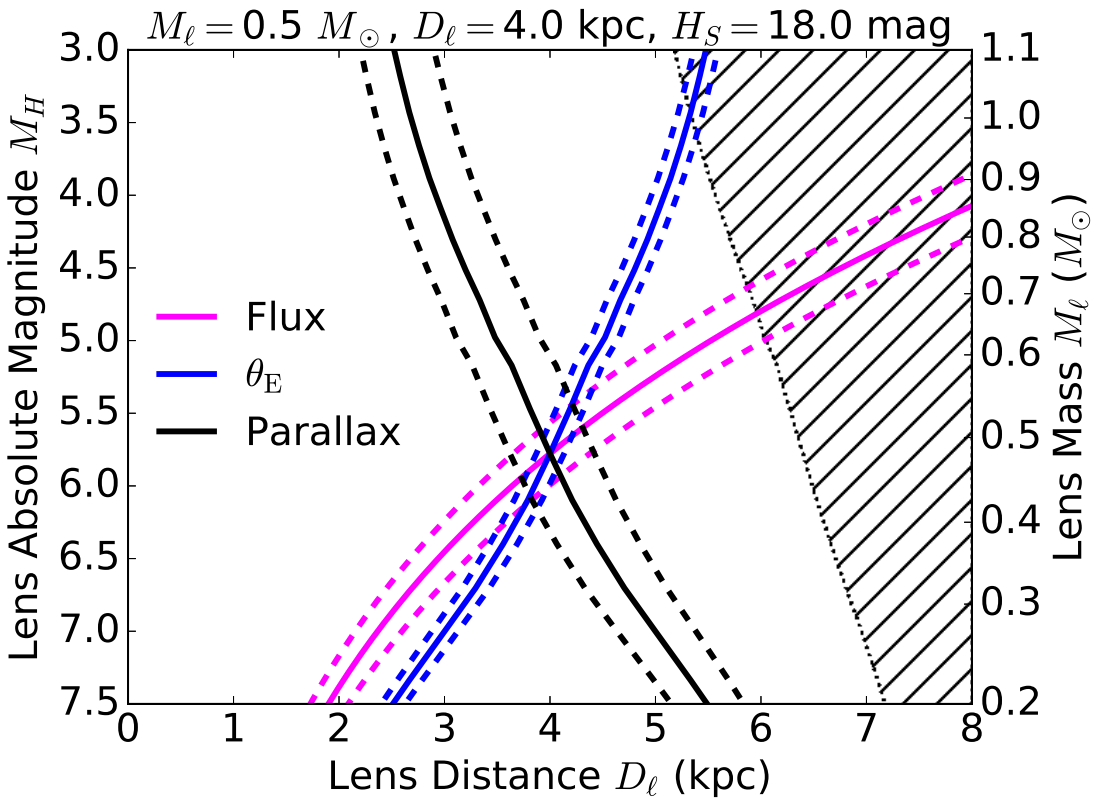

Figure 2 The absolute H-band magnitude, M_H, and mass, M_ℓ, of an isolated lens star as a function of its distance D_ℓ as constrained by measurements of the Einstein radius $\theta_{\rm E}$ (blue line), the lens flux F_ℓ (pink), and the microlensing parallax $\pi_{\rm E}$ (black), assuming the source star has an apparent H-band magnitude of $H_s = 18$, and that $D_\ell = 4$ kpc and $M_\ell = 0.5\ M_\odot$. Any two of these techniques will provide a unique solution for D_ℓ and M_ℓ, with all three yielding an independent verification.

Theme 7: Properties of the *WFIRST* Microlensing Mission

Campaigns:

- *WFIRST* observes at quadrature, with the middle of the seasons approximately at the Equinoxes. This is due to the combination of sun angle constraints and the fact that the bulge is at (RA, Dec) $\sim$ (18h, -30°).
- Each campaign will be 72 continuous days at a $\sim$15 minute cadence
- There will be six campaigns, probably spaced as two in the first year (spring and fall), two in the fifth year (spring and fall), and two at some point in the middle (either in spring or fall).

Field:

- camera is 0.28 deg^2
- pixel scale is 0.11"
- Original plan was for 10 fields toward (l, b) $\sim$ (0.5, -1.5)
- Primary filter is W149 (wide $\sim H$-band); secondary filter is Z087

References

Dominik, M., & Sahu, K. C. 1998, ArXiv Astrophysics e-prints, astro-ph/9805360

Han, C., & Jeong, Y. 1999, MNRAS, 309, 404

Lu, J. R., Sinukoff, E., Ofek, E. O., Udalski, A., & Kozlowski, S. 2016, ApJ, 830, 41